

FABRICATION AND CHARACTERIZATION OF Al 7075 HYBRID COMPOSITE REINFORCED WITH GRAPHENE AND SiC NANOPARTICLES BY POWDER METALLURGY

X. M. DU*, K. F. ZHENG, T. ZHAO, F. G. LIU

School of Materials Science and Engineering, Shenyang Ligong University, Shenyang 110159, China

Processing of Al7075 matrix composites reinforced with content (1.0 wt.%) of graphene and SiC nanoparticles (0.25-2.0 wt.%) using ball milling and vacuum hot press is reported. Near full densification was observed for all the composite compositions at the sintering temperature of 610°C (time of 1.5 h and applied pressure of 50 MPa). Detailed analysis of the microstructure and mechanical and tribological properties with reinforcement content in Al7075-graphene-SiC_pcomposites is presented. The results show that the graphene and SiC nanoparticles predominantly are homogeneously distributed on the grain boundaries of Al matrix and SiC nanoparticles are distributed between graphene sheets. There is a significant increase in the hardness and wear resistance and a reduction in the coefficient of friction values compared to pure Al7075 alloy.

(Received August 18, 2018; Accepted November 28, 2018)

Keywords: Microstructure, Wear, Aluminum hybrid composites, Graphene, SiC nanoparticles

1. Introduction

Aluminum (Al) based metal matrix composites (MMCs) have been extensively studied as an attractive choice of automotive, aerospace and military applications due to their light-weight, high strength, stiffness and resistance to high temperature [1]. Generally, the micro-ceramic particles (such as Si₃N₄, BC₄, SiC, TiN, BN, MgO and Al₂O₃ etc) are used to improve the yield and ultimate strength of the metal [2-5]. However the ductility of the MMCs deteriorates with high ceramic particle concentration. Nano-structural reinforcements (particulate, fiber and sheet etc.) can significantly enhance the mechanical strength of the matrix by more effectively promoting the strengthening and toughening mechanisms than micron size reinforcements [6].

Lot of work has been carried out to prepare aluminum matrix composites reinforced with the single nano reinforcements for enhancing the mechanical strength of the aluminum matrix. El-Eskandarany [7] prepared SiC particle reinforced aluminum matrix nanocomposites using high-energy ball milling for homogeneous mixing of the SiC and Al powders. Prabhu and co-workers [8] prepared homogenous Al-Al₂O₃ nanocomposite powders by high-energy milling. Sahebet *al.* [9] synthesized carbon nanotube(CNT) reinforced Al6061 and Al2124 alloy based nanocomposites with uniform dispersion of CNTs through sonication and ball milling technique.

Wang et al [10] reported that the tensile strength of Aluminum composite reinforced with only 0.3 wt-% graphene nanosheets by powder metallurgy is 249 MPa. It was 62% enhancement over the unreinforced aluminum matrix. Li et al.[11] reported that the aluminum composite reinforced with only 0.3 wt.% of graphene oxide shows an 18% and 17% increase in elastic modulus and hardness, respectively, over unreinforced aluminum. Yan Shao-jiu et al.[12] reported that the tested tensile strength and yield strength of 0.3 wt% graphene-reinforced aluminum matrix composites fabricated by powder metallurgy, compared to the pristine aluminum alloy, show an increase of 25% and 58%, respectively. Kumar et al. [13] reported about the effect of graphene reinforcement on the tribological aspects of aluminum matrix composites.

But there is not much literatures found on hybrid composites in combination with graphene and ceramic particles so far. Siddhartha et al. [14] reported the preparation of Al 6061

*Corresponding author: du511@163.com

matrix nanocomposites reinforced with graphene flake and SiC particle by powder metallurgy. The hardness of composites superior to the Al 6061 matrix. Kumar et al. [15] prepared Al 356 alloy/ (graphene + SiC) hybrid composites with different hybrid ratios using semisolid stirring assisted ultrasonic cavitation method. The ultimate tensile strength and yield strength of the nanocomposites with addition of 5 wt.% graphene and 5 wt.% micro SiC particles improved by 47% and 34%, respectively. However, the toughness of hybrid reinforced aluminum matrix composites has not been reported in these literatures.

This work is carried out to study the effect of the SiC nanoparticles and graphene sheets addition in the Al7075 alloy. Ball milling dispersion method is carried out to avoid the agglomeration of graphene and SiC nanoparticles. Thus prepared powder mixtures are compacted and sintered. The effects of SiC nanoparticles addition with different content on microstructure and mechanical properties of Al7075-graphene-SiC composites are discussed.

2. Experimental procedures

Al7075 hybrid metal matrix composites (Al7075-graphene-SiC_p) was prepared by powder metallurgy. Al7075 is a matrix material. SiC nanoparticles and graphene are the reinforcing elements. The Al7075aluminum alloy with 1.0wt. % of graphene and 0.25, 0.5, 1.0, 1.5 and 2.0wt.% of SiC nanoparticles was prepared by powder metallurgy. Al7075 alloy powder (10 μ m, supplied from Beijing Hongyu Materials Company), a sufficient amount of α -SiC nanoparticle (800 nm, supplied from Shanghai Yunfu Nanotechnology Co., Ltd.) and pure pristine multilayer graphene with the average lateral size of 5 μ m (supplied from Nanjing XFNANO Materials Tech Co.,Ltd) were used.

At the first step, calculated quantity of Al7075 powder and graphene were mixed into a mixture. Further, SiC nanoparticle with various weight percentage (0.25, 0.5, 1.0, 1.5 and 2.0 wt. %) were added to graphene-Al7075 mixture to perform ball milling, respectively. The ball milling was performed for 6 hours with a speed of 50 r/min and ball-to-powder ratio of 5:1 using tungsten carbide jar and balls. The powder mixtures were then consolidated in vacuum hot press at 610°C for 1.5 hours under a pressure of 50 MPa using high temperature lubricants such as boron nitride between the punch and die walls. Heat-resistant steel dies and punches were used to sinter 50 mm-diameter and 15 mm-thick compacts of each composition.

The sintered composites are machined into samples with dimensions of 45 mm \times 10 mm \times 2.0mm and then subjected to solutionizing at a temperature of 475°C for 2 hours followed by quenching using cold water. The quenched samples are then subjected to artificial aging for 24 hours at a temperature of 135°C.

X-ray diffraction analysis on polished samples were carried out by X-ray diffraction (Rigaku Ultima IV), using Cu K α radiation for 20-90degrees. Raw XRD data were refined and analyzed via MDI Jade 6.0 program (Materials Data Incorporated: Livermore, CA, USA). The surface morphology was observed by a scanning electron microscopy (SEM) of TESCAN equipped with energy-dispersive spectrometer (EDS) and an optical microscope (OM) of Carl Zeiss Axiovert200MAT.

Hardness measurements of composite samples were carried out on a Vickers hardness testing machine (Shanghai Shuangxu, Inc., HVS-50, China), using a load of 9.8 N, and the mean values of at least five measurements conducted on different areas of each sample was considered.

Dry sliding wear tests were carried out on the composites at ambient laboratory conditions by a universal friction and wear testing machine (Jinan Jingcheng, Inc., MMW-1A, China). The test material in the form of pins of diameter 16mm and height 10mm were slid against a rotating steel ring (counter face) with a hardness of 62 HRC, having the diameter of 10mm and thickness of 10 mm. Specimens were subjected to an initial run-in period until the whole surface of the pin was in full contact with the ring surface. They were then ground with 800 grit silicon carbide paper, cleaned in an ultrasonic bath with acetone for 6 min and hot wind dried below 100°C. Wear tests were undertaken under the normal load of 40N, the rotating speed of steel ring of 60 r/min and the test time of 60 minutes. For each wear test, the wear weight loss was measured after 10 min intervals for total test duration of 60 minutes. At least three wear tests were performed. Coefficient of friction (COF) during wear tests was also recorded for each test. The surface profile of the wear tracks was analyzed using a laser scanning confocal microscopy (LSCM) (LEXT OLS4100, Japan).

3. Results and discussion

3.1. Microstructure

X-ray diffraction investigations were carried out to identify the phases presented in the composite samples with various nano-SiC particles, and the results were illustrated in Fig. 1. It could be seen that most of the peaks corresponding to Al were identified in these XRD patterns. In these composite samples it can be seen that besides Al reflections, there appeared a broad peak at about $2\theta = 43^\circ$ and some smaller peaks indicating the graphene and SiC nanoparticles. The broad peaks are formed from the metastable hexagonal η (MgZn_2) phase [16]. The smaller peaks at $2\theta = 26.5^\circ$ and $2\theta = 35.8^\circ$, 60.1° and 72° indicate the presence of graphene and SiC particles, respectively and conclude that uniform structure was formed in Al 7075 alloy. As also seen from Fig. 1, the intensity of SiC_p peaks increased with the content of SiC_p , and this indicated that the SiC_p entered into the 7075 Al matrix. Several studies have reported formation of aluminum carbide (Al_4C_3) at the high surface energy prismatic planes of carbon exposed by defects [17]. In this analysis, aluminum carbide (Al_4C_3) peaks were not found, indicating better potential of graphene in strengthening Al based composites.

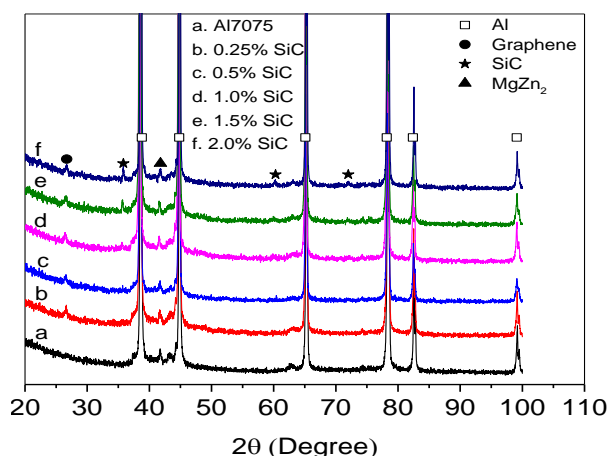


Fig.1 XRD patterns of Al7075 and Al7075-graphene- SiC_p composites.

Fig. 2 shows the optical micrographs of the pure Al7075 and the composites with graphene and various SiC nanoparticles. As seen from Fig. 2, in the pure Al 7075 (Fig. 2(a)), there is only a very small amount of pores, and the average size of Al 7075 grains is about $10\ \mu\text{m}$. In the Al7075-graphene- SiC_p composites, it clearly shows the formation of refined and small grains compare to monolithic alloy. Fig. 2 (b)-(f) show the distribution of reinforcements on the matrix material. Graphene and SiC_p have uniformly distributed on the aluminum composites and mostly particles are in grain boundaries. No particle agglomeration is observed.

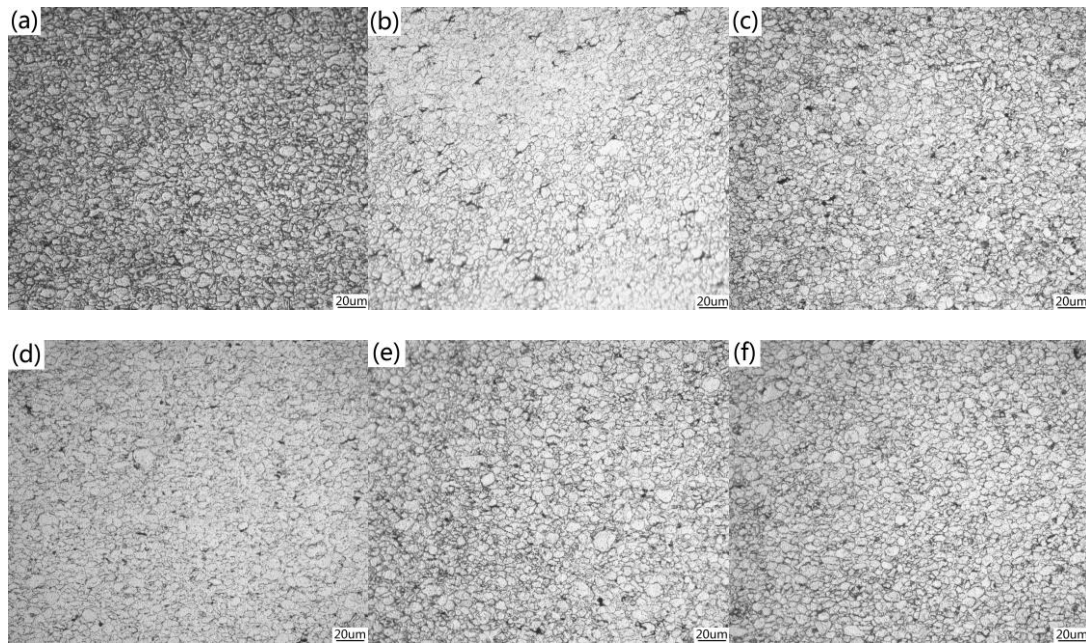


Fig. 2. The OM micrographs: (a) the pure Al7075 alloy, (b) Al7075-graphene-0.25 wt.% SiC_p, (c) Al7075-graphene-0.5 wt.% SiC_p, (d) Al7075-graphene-1.0 wt.% SiC_p, (e) Al7075-graphene-1.5 wt.% SiC_p, (f) Al7075-graphene-2.0 wt.% SiC_p composites.

The SEM micrographs were taken at high resolution in order to verify the dispersion of graphene and nano SiC particles. Fig. 3 shows the SEM micrographs of the composites with graphene and nano SiC particles. The graphene and nano SiC_p are reasonably distributed within Al matrix and no cluster of nanoparticles is observed in the micrographs for all samples. It can be also found that the graphene and SiC_p predominantly are distributed on the grain boundaries of Al matrix (Fig. 3 (b) and (d)). Fig. 3 (f) shows the local magnification in Fig. 3 (c). It can be clearly found that SiC particles are distributed between graphene sheets, which is beneficial to improving the wettability between SiC particles and Al matrix. Generally, nano-scalar particles have a high propensity to agglomerate at grain boundaries during preparing metal matrix composites by powder metallurgy or stirring casting methods. This is attributed to the difference of the thermal conductivity of the particles and metal matrix. Khan and Rohatgi [18] showed that when the thermal conductivity of the particle is greater than that of the melt, the particles can be engulfed in the matrix instead of agglomeration at grain boundaries. Many studies have proposed surface modification technology of ceramic particles to adjust the surface thermal conductivity of particles, such as copper plating and surface deposition etc. These techniques reduce particle agglomeration to a certain extent. However, the composition of the composite is also affected by the adverse effects, thereby affecting the properties of the composites. SiC nanoparticles are sandwiched in graphene sheets, which significantly improved their surface thermal conductivity. This helps to avoid the aggregation of SiC particles at the grain boundaries. Boostani et al. [19] prepared the aluminum matrix composites reinforced with SiC nanoparticles encapsulated by onion-like graphene shells using mill balling and stirring casting methods. It was found that SiC nanoparticles dispersed homogeneously throughout the aluminum matrix.

As seen in Fig. 3, with the increase of SiC_p content, more and more phases, including external reinforcements (nano SiC_p and graphene) and endogenous precipitates (η' phase), are distributed at grain boundaries. EDS analysis of the rectangular area in Fig. 3 (f) was performed, and the results are shown in Fig. 3 (g). It is found that these phases at the grain boundaries contain a large amount of carbonaceous composition and a small amount of Si, Cu, Zn and Mg elements. It supplied evidence of the existence of graphene and SiC_p at grain boundaries in the composites.

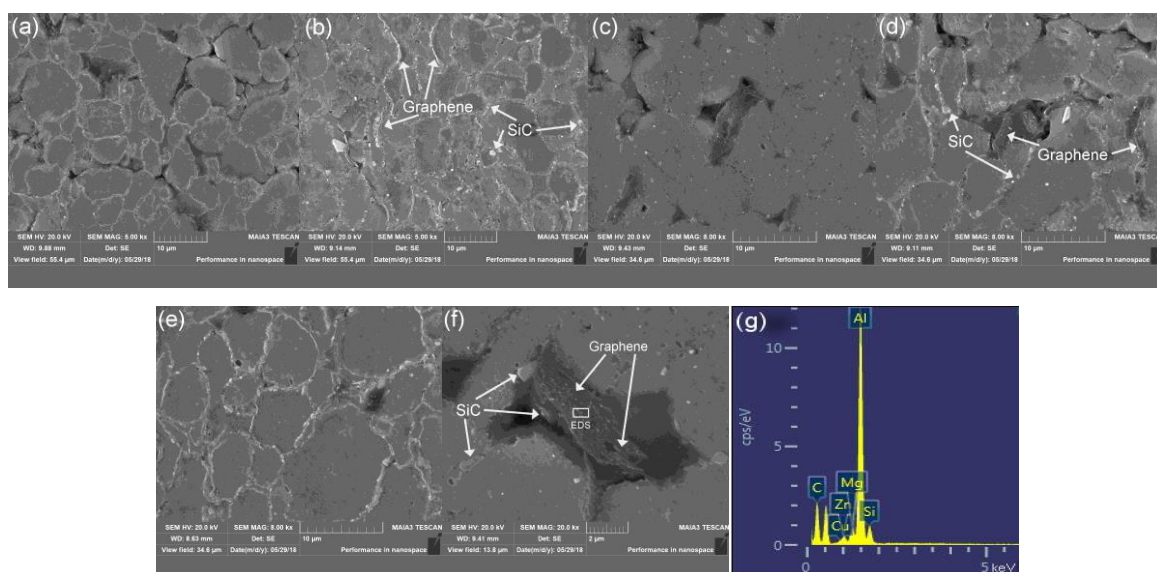


Fig. 3. The SEM micrographs: (a) Al7075-graphene-0.25 wt.% SiC_p, (b) Al7075-graphene-0.5 wt.% SiC_p, (c) Al7075-graphene-1.0 wt.% SiC_p, (d) Al7075-graphene-1.5 wt.% SiC_p, (e) Al7075-graphene-2.0 wt.% SiC_p composites, (f) the local magnification in (c), (g) the EDS of the selected area in (f).

3.2. Mechanical properties

Microhardness values were measured for Al7075 alloy and various concentrations of SiC_p in Al7075-graphene-SiC_p composites. The results are summarized in Fig. 4. With the increase of the nano SiC_p contents, the microhardness of the composites improves. The microhardness of Al7075 alloy sample is 92.0 ± 4.6 HV. While the microhardness of Al7075-graphene-2.0 wt.% SiC_p composite is 158 ± 7.9 HV, showing 71.7% increments over the unreinforced aluminum under otherwise identical experimental conditions. It can be explained that nano-structured graphene and SiC_p can inhibit grain growth in aluminum matrix through grain boundary pinning and therefore lead to a finer grain structure of aluminum. Finer grain structures can result in higher microhardness values.

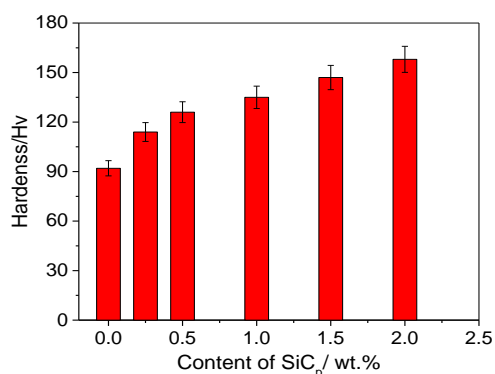


Fig. 4. The microhardness of Al7075 alloy and the composites.

Fig. 5 shows the wear loss (g) of pure Al 7075 and Al 7075-graphene-SiC_p composites with various weight percentage of nano SiC_p. It is indicated that upon addition of graphene and nano SiC_p the wear loss decreases continuously with increasing nano SiC_p content. This trend is consistent with the increase in microhardness observed for these composites (Fig. 4). The reinforcing SiC_p increased the wear resistance and

caused the wear loss of the composite surface to be lower compared with main materials. Further, while increasing the SiC_p content significant decrease in the wear loss was observed. This extensive reduction in the wear loss is attributed to the strengthening of composites by an addition of graphene and SiC_p [14,15] and its tribological properties which forms the thin dry lubricant layer between mating metal. This behavior is in consistent with the work done by the other researchers [20, 21]. Nano SiC_p in the region of this work resulted in improvement in wear resistance. SiC has very high hardness ($\sim 2840\text{-}3240$ HV), and its reinforcement in softer materials such as Al increases the hardness of the composite. The Al7075-graphene- SiC composites exhibited higher microhardness compared to pure Al7075 alloy (Fig. 4). The improved wear resistance of these composites is consistent with the Archard's law that states that wear volume loss is inversely proportional to the hardness of the material being worn away.

The variation in the measured average coefficients of friction with the weight percentage of SiC_p in the composites also was shown in Fig. 5. It is indicated that there is a decrease in the average coefficients of friction for an increase in SiC_p content in the composite compared to that of Al 7075 base alloy. The average coefficients of friction for Al 7075 composites are found to be 0.24-0.31, which is very less compared to Al 7075 base alloy (0.39). A reduction of 20.5% to 36.3% in average coefficient friction is observed for composites containing 0.25 wt.% to 2.0 wt.% SiC_p , when compared with the matrix Al 7075 alloy. Uvaraja et al. [22] reported that the average coefficient of friction were in the range of 0.33 and 0.35 for Al 7075 composites reinforced with 5-15 wt. % SiC particles and a reduction of 17.24%, 20.83% and 27.27% in average friction coefficient for composites containing 5 wt.%, 10 wt.% and 10 wt.% SiC_p compared with the matrix Al 7075 alloy. It is clearly found that the addition of graphene and nano SiC particles to Al 7075 matrix is more effective to reduce the coefficient of friction of composites than that of single micrometer SiC particles. The composites have better antifriction properties. This can be mainly attributed to the excellent lubricating properties of graphene. In general, the coefficient of friction depends on the mating materials and relative hardness. Further, the decrease in the coefficient of friction is attributed to the formation of graphene solid lubricant layer between the wear surfaces which gives rise to the smooth surface thereby reducing the contact area. Moreover, the addition of graphene to aluminum matrix can greatly reduce the amount of SiC particles, which is beneficial to the improvement of the toughness of composites.

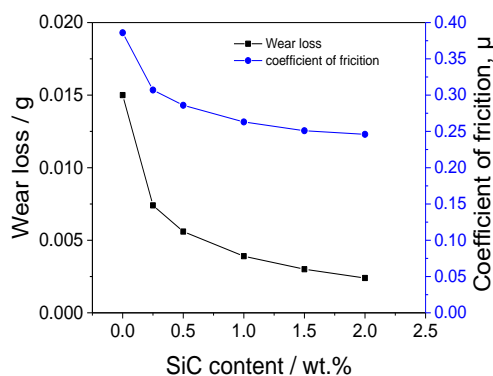


Fig. 5. Wear loss and coefficient of friction Al 7075 and the composites with varying the SiC_p content.

In order to investigate the wear mechanism, the surfaces of the worn samples were examined under laser scanning confocal microscopy (LSCM). Fig. 6 shows typical worn surfaces of the pure Al 7075 alloy and Al 7075-graphene- SiC_p composites. The pure Al7075 has a smooth surface nature with more tribolayers formed (Fig. 6(a)). Hence, the wear rate is more in unreinforced sample. However, the worn surface of the composites is generally much rougher than that of the unreinforced alloy (Fig. 6(b-f)). The Al7075 based composites reinforced with graphene and nano- SiC_p show more cavities and micro-grooves on the worn surface after wear as shown in Fig. 6(b-f). Micro-grooves are mainly formed by the nano- SiC_p in the matrix. As the weight percentage of nano- SiC_p increases, the number of grooves increases and the nano- SiC_p are projecting out from the pin surface due to ploughing action between the counterface pin. The hard particles are found inside the cavities. This indicates an abrasive wear mechanism which is essentially a result of hard particles and resist the delamination process, so that the wear resistance is good in case of aluminum matrix composite.

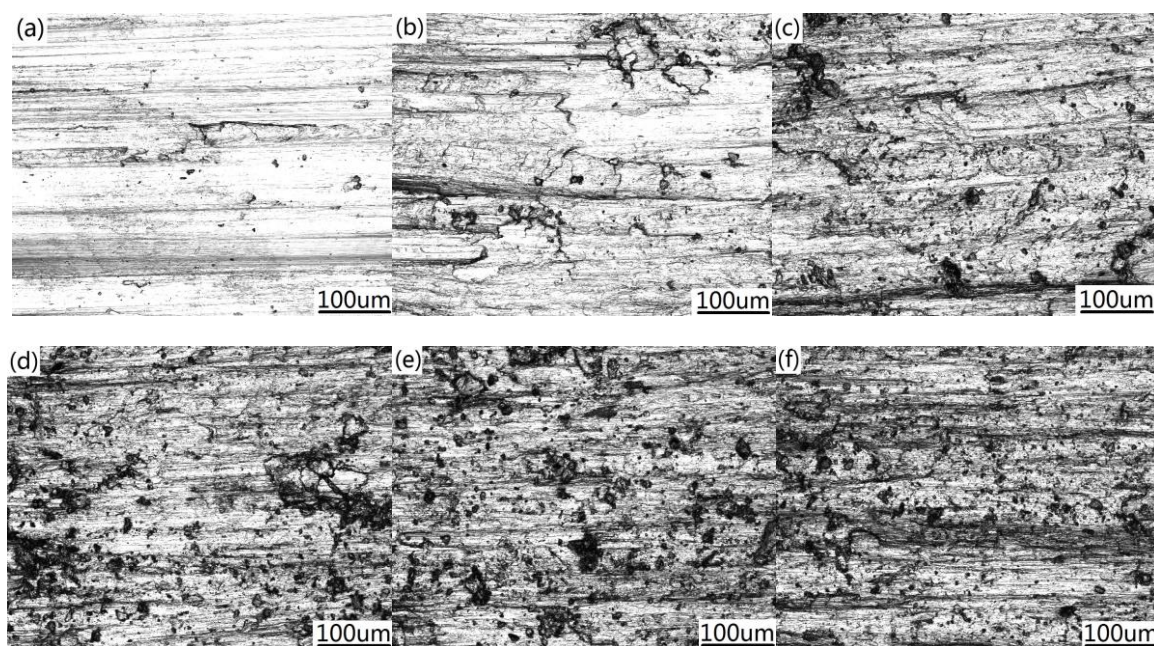


Fig. 6. Morphologies of worn surfaces of unreinforced alloy and composites, (a) Al7075, (b) Al7075-graphene-0.25 wt.% SiC_p, (c) Al7075-graphene-0.5 wt.% SiC_p, (d) Al7075-graphene-1.0 wt.% SiC_p, (e) Al7075-graphene-1.5 wt.% SiC_p, (f) Al7075-graphene-2.0 wt.% SiC_p composites.

4. Conclusions

Al7075 matrix composites reinforced with 1.0 wt.% content of graphene and SiC nanoparticles (0.25-2.0 wt.%) have been successfully processed by ball milling and vacuum hot press. X-ray diffraction analysis shows the presence of the carbon and silicon carbide peaks and no proof for formation of aluminium carbide. SEM analysis shows that the graphene and SiC nanoparticles predominantly are homogeneously distributed on the grain boundaries of Al matrix and SiC nanoparticles are distributed between graphene sheets. Al7075 composites exhibited higher microhardness than pure Al7075 alloy.

The microhardness increased by about 71.7% with the reinforcement of 2.0 wt.% SiC and 1.0 wt.% graphene. Consistent with the microhardness improvements, marked improvements in wear resistance was observed with the reinforcement of graphene and SiC nanoparticles in the composites. On increasing the SiC nanoparticles content, the wear loss and coefficient of friction values were reduced. A reduction of 20.5% to 36.3% in average coefficient friction is observed for composites containing 0.25 wt.% to 2.0 wt.% SiC_p, when compared with the matrix Al 7075 alloy. Due to the presence of favourable tribological properties, Al 7075-graphene-SiC_p composite may be considered as an excellent candidate for various applications where the component is exposed to wear and friction.

Acknowledgment

This work is supported by Shenyang Science and Technology Project (No.18-013-0-33) and Shenyang Youth Science and technology innovation support program and the Natural Science Foundation of Liaoning (2015602642) in Liaoning Province, China.

References

- [1] Yashpal, Sumankant, C.S. Jawalkar, A. S. Verma, N.M. Suri, *Materials Today: Proceedings* **4**, 2927 (2017).

- [2] P. S. Bains, S. S. Sidhu, H. S. Payal, *Mater. Manuf. Process.* **31**, 553 (2016).
- [3] J. Singh, A. Chauhan, *J. Mater. Res. Technol.* **5**, 159 (2016).
- [4] A. Mortensen, J. Llorca, *Annu. Rev. Mater. Res.* **40**, 243 (2010).
- [5] B. S. Yigezu, P. K. Jha, M. M. Mahapatra, *Mater. Manuf. Process.* **28**, 969 (2013).
- [6] S. M. Choi, H. Awaji, *Sci. Technol. Adv. Mater.* **6**, 2 (2005).
- [7] M. S. E. Eskandarany, *J. Alloys Compd.* **279**, 263 (1998).
- [8] B. Prabhu, C. Suryanarayana, L. An, R. Vaidyanathan, *Mater. Sci. Eng. A* **425**, 192 (2006).
- [9] N. Saheb, T. Laoui, N. Al-Aqeeli, M. A. Atieh, A. Al-Qutub, *Development of Aluminum Based Nanocomposites through Powder Metallurgy and Novel Sintering Technologies for Structural and Tribological Applications; ARP-28-122, Final Report; King Abdulaziz City for Science and Technology: Riyadh, Saudi Arabia, 2013.*
- [10] J. Wang, Z. Li, G. Fan, H. Pan, Z. Chen, D. Zhang, *Scripta Materialia* **66**, 594 (2012).
- [11] Z. Li, G. Fan, Z. Tan, Q. Guo, D. Xiong, Y. Su, Z. Q. Li, D. Zhang, *Nanotechnology* **25**, 325601 (2014).
- [12] S. J. Yan, Y. Cheng, H. Q. Hu, C. J. Zhou, L. D. Bo, D. S. Long, *J. Mater. Eng.* **4**, 1 (2014).
- [13] H. G. Prashantha Kumar, M. Anthony Xavier, *Tribology - Materials, Surfaces & Interfaces* **11**, 88 (2017).
- [14] J. Siddhartha, K. H. G. Prashantha, M. X. Anthony, *IOP Conf. Series: Materials Science and Engineering* **149**, 012086 (2016).
- [15] K. A. Praveen, S. Aadithya, K. Dhilepan, N. Nikhil, *ARPN Journal of Engineering and Applied Sciences* **11**, 1204 (2016).
- [16] Y. H. Zhao, Z. X. Liao, Z. Jin, R. Z. Valiev, Y. T. Zhu, *Min. Meta. Mater. Soc.* **4**, 511 (2004).
- [17] S. F. Bartolucci, J. Paras, M. A. Rafiee, J. Rafiee, S. Lee, D. Kapoor, N. Koratkar, *Mater. Sci. Eng. A* **528**, 7933 (2011).
- [18] M. A. Khan, P. K. Rohatgi, *Compos. Eng.* **3**, 995 (1993).
- [19] A. F. Boostani, S. Tahamtan, Z. Y. Jiang, D. Wei, S. Yazdani, R. A. Khosroshahi, R. T. Mousavian, J. Xu, X. Zhang, D. Gong, *Composites: Part A* **68**, 155 (2015).
- [20] R. J. Young, I. A. Kinloch, G. Lei, K. S. Novoselov, *Compos. Sci. Technol.* **72**, 1459 (2012).
- [21] J. Lin, L. Wang, G. Chen, *Tribol. Lett.* **41**, 209 (2011).
- [22] V. C. Uvaraja, N. Natarajan, K. Sivakumar, S. Jegadheeshwaran, S. Sudhakar, *Indian Journal of Engineering and Materials Sciences* **22**, 51 (2015).